ANTIOXIDANTS & REDOX SIGNALING
Volume 9, Numbers 7, 2007

DOI: 10.1089/ars.2007.1509

Original Research Communication

Acid Sphingomyelinase and Its Redox Amplification in Formation of Lipid Raft Redox Signaling Platforms in Endothelial Cells

ANDREW Y. ZHANG,[1–3] FAN YI,[1,3] SI JIN,[1] MIN XIA,[1] QI–ZHENG CHEN,[1] ERICH GULBINS,[2] and PIN–LAN LI[1]

ABSTRACT

This study examined the role of acid sphingomyelinase (ASM) and its redox amplification in mediating the formation of lipid raft (LR) redox signaling platforms in coronary arterial endothelial cells (CAECs). Using small interference RNA (siRNA) of ASM, Fas ligand (FasL)-induced increase in ASM activity, production of ceramide, and LR clustering in CAECs were blocked, and clustered Fas was also substantially reduced in detergent-resistant membrane fractions of CAECs. LR clustering, $gp91^{phox}$ aggregation, and $p47^{phox}$ translocation to the LR clusters induced by FasL were also blocked in ASM-siRNA transfected CAECs. Corresponding to this reduction of LR clustering with NAD(P)H oxidase subunits in ASM-siRNA transfected CAECs, superoxide ($O_2^{-\bullet}$) production was significantly decreased as measured by either ESR or fluorescent spectrometry. Interestingly, superoxide dismutase (SOD) not only scavenged $O_2^{-\bullet}$, but also markedly attenuated LR clustering. Xanthine/xanthine oxidase, an exogenous $O_2^{-\bullet}$ generating system, dramatically increased ASM activity and LR clustering in EC membrane and enhanced FasL-induced LR clustering, which were blocked by SOD. These results suggest that that ASM activates LR clustering to form redox signaling platforms, where $O_2^{-\bullet}$ production enhances ASM activity, and thereby results in a forwarding amplification of LR and redox signaling. This ASM-mediated feedforwarding mechanism may be critical for an efficient transmembrane signaling through LRs. *Antioxid. Redox Signal.* 9, 817–828.

INTRODUCTION

THERE IS INCREASING evidence that clustering of distinct cholesterol- and sphingolipid-rich membrane rafts [lipid rafts (LRs)] is importantly involved in transmembrane signaling in a variety of mammalian cells (10, 22, 23, 34). Many receptors including tumor necrosis factor α (TNF-α) receptors, Fas, DR3, 4, 5, insulin receptors, and integrins, as well as other signaling molecules, can be aggregated within the LR clusters to form signaling platforms (6, 13, 27, 44). The formation of these LR signaling platforms with aggregation of different signaling molecules may represent one of important mechanisms determining the variety of transmembrane signaling, and it also robustly amplifies signals from activated receptors. Previous studies have reported that the formation of LR signaling platforms in the cell membrane has been implicated in the regulation of cell or organ functions through its effect on various biological processes including cell growth, differentiation and apoptosis, T-cell activation, tumor metastasis, and neutrophil and monocyte infiltration (17, 33, 44). Recently, we reported that LR clustering importantly participates in the development of endothelial dysfunction in

[1]Department of Pharmacology and Toxicology, Medical College of Virginia Campus, Virginia Commonwealth University, Richmond, Virginia.
[2]Department of Molecular Biology, University of Essen, Essen, Germany.
[3]Equally contributes to this work.

coronary arteries, which is associated with the formation of LR redox signaling platforms (44). These signaling platforms in the membrane of coronary arterial endothelial cells (CAECs) are characterized by gp91^{phox} and p47^{phox} aggregation in LR clusters and enhanced NAD(P)H oxidase activity, when the cells were stimulated by different death receptor ligands. However, the mechanism mediating the formation these endothelial LR redox signaling platforms remains unclear.

Fas ligand (FasL) primarily activates acid sphingomyelinase (ASM), rather than neutral sphingomyelinases (NSM), and that activation of ASM is importantly involved in the development of endothelial dysfunction (42). The present study hypothesized that ASM is a key enzyme responsible for the formation of LR redox signaling platforms in coronary endothelial cells. In this way, ASM or its product, ceramide, initiates or promotes the formation of LR platforms by formation of ceramide-enriched microdomains. These ceramide-enriched microdomains could spontaneously fuse to form larger ceramide-enriched platforms or clusters under certain conditions (13, 14, 17, 18), where NAD(P)H oxidase is assembled to produce redox molecules (44). On the other hand, recent studies have shown that $O_2^{-\bullet}$ or other ROS can also alter ceramide level in cells through their action on sphingomyelinase (SM) and ceramidase (1, 26, 31). It would be interesting to know what are the relationships between both signaling pathways and how they influence each other. A recent study has reported that ASM may be dimerized and thereby largely activated by oxidants (31). This led us to wonder whether there is a feedforwarding mechanism through ASM in the endothelial LR redox signaling platforms, where $O_2^{-\bullet}$ enhances AMS activity and further promotes LR clustering, resulting in intrinsic signaling amplification in the platforms.

To test this hypothesis, we first determined the role of ASM in LR clustering and associated trafficking or aggregation of Fas and NAD(P)H oxidase subunits, gp91^{phox} and p47^{phox}. Then we tested whether a redox feedforwarding mechanism via ASM is involved in the formation of these LR redox signaling platforms.

MATERIALS AND METHODS

Cell culture

Fresh bovine hearts were obtained from a local abattoir and were immediately transported to the laboratory. The epicardial circumflex and anterior descending coronary arteries were quickly dissected and placed in RPMI 1640 supplemented with 5% fetal calf serum (FCS), 2% antibiotic–antimycotic solution, 0.3% gentamycin, and 0.3% nystatin, and cleaned of surrounding adherent fat and connective tissue. The lumen of arterial segments was filled with 0.25% collagenase A in RPMI 1640 supplemented with 0.1% bovine serum albumin (BSA) and incubated at 37°C for 15–30 min. The arteries were then flushed with RPMI 1640 supplemented with 2% antibiotic–antimycotic solution, 0.3% gentamycin, and 0.3% nystatin. Detached bovine CAECs were collected and maintained in RPMI 1640 supplemented with 20% FCS, 1% glutamine, and 1% antibiotic–antimycotic solution at 37°C in 5% CO_2. CAECs were identified by morphological appearance (*i.e.*, cobblestone array) and by positive staining for von Willebrand factor antigen. All biochemical studies were performed using CAECs of two to four passages.

RNA interference

Small interference RNAs (siRNAs) were purchased from Qiagen (Valencia, CA). The DNA target sequence for ASM-siRNA is: 5′-AAGGCCGTGAGTTTCTACCT-3′ and for NSA-siRNA is: 5′-AAGCGCTGGGAGACTTTCTA3′. The scrambled small RNA (AATTCTCCGAACGTGTCACGT) has been confirmed as nonsilencing double-stranded RNA and was used as control in the present study. In these experiments, siRNA transfection was performed according to the manufacturer's instruction in Qiagen TransMessenger kit. All siRNAs were chosen with a Qiagen siRNA design program and synthesized by Qiagen. The transfection efficiency was examined by a parallel transfection using a scrambled mRNA labeled with fluorescein and detection of mRNA and protein expression levels of targets.

RNA isolation and real-time RT–PCR analysis

Total RNA was isolated from ECs using TRIzol reagent (GIBCO, Life Technologies, Carlsbad, CA) according to the protocol described by the manufacturer. The mRNA levels for target genes were analyzed by real-time quantitative RT–PCR using a Bio-Rad iCycler system (Bio-Rad, Hercules, CA) according to the protocol described by the manufacturer. The mRNA levels of ASM and NSM were normalized to the 18S mRNA. Primers for ASM are: (forward) 5′-CCGAGA CACCCAATCAGATAGC-3′ and (reverse) 5′-CAGGTCAGAGATGTGCCAGAAC-3′. Primers for NSM are: (forward) 5′-CATGATGCCTATACTGGAGACC-3′ and (reverse) 5′-CATGATGCCTATCT GGAGACC-3′. Primers for 18S are: (forward) 5′-GCGCTAGACTCCGAGAACAT-3′ and (reverse) 5′-TGGCCA CTTACTACCTGACC CTT-3′.

Sphingomyelinase assay

The activity of sphingomyelinase was determined as reported (40) . Briefly, *N*-methyl-[^{14}C]-sphinomyelin was incubated with cell homogenates, and the metabolites of sphingomyelin, [^{14}C]-choline phosphate and ceramide, were quantified. For ASM, an aliquot of homogenates (20 μg) was mixed with 0.02 μCi of *N*-methyl ^{14}C-sphingomyelin in 100 μl acidic reaction buffer containing 100 mmol/L sodium acetate, and 0.1% Triton X-100, pH 5.0, and incubated at 37°C for 15 min. The reaction was terminated by adding 1.5 ml chloroform:methanol (2:1) and 0.2 ml double-distilled water. The samples were then vortexed and centrifuged at 1,000 *g* for 5 min to separate into two phases. A portion of the upper aqueous phase containing ^{14}C-choline phosphate (ceramide in lower organic phase) was transferred to scintillation vials and counted in a Beckman liquid scintillation counter. The choline phosphate formation rate (pmol·min^{-1}·mg protein^{-1}) was calculated to represent the enzyme activity.

Ceramide assay

Lipids from CAECs were extracted as described previously (42). DAG kinase assay was used in this study to measure the

ceramide level as reported (40). Briefly, the dried lipids were solubilized into a detergent solution containing 7.5% *n*-octyl-β-D-glucopyranoside, and 5 mmol/L cardiolipin in 1 mmol/L diethylenetriaminepentaacetic acid (DETAPAC) solution, and then mixed with 4 μg DAG kinase (Calbiochem, San Diego, CA) and 4 μCi [γ-^{32}P] ATP to a final volume of 100 μl. After incubation at 25°C for 3 h, the reaction was stopped by extracting the lipids with 600 μl chloroform:methanol (1:1, vol/vol), 20 μl 1% perchloric acid, and 150 μl 1 mol/L NaCl. The lower organic phase was recovered and dried with N_2. The ^{32}P-labeled Cer-1-P was separated from other lipids by thin layer chromatography (TLC) with a solvent consisting of chloroform:acetone: methanol:acetic acid:water (10:4:3:2:1, vol/vol/vol/vol/vol). After visualization by autoradiography, the ceramide-1-^{32}P band was recovered by scraping and counted in a scintillation counter. The phosphorylation of C_6-ceramide as an internal control was determined in parallel. The identity of ceramide was confirmed by HPLC analysis as reported previously. The ceramide concentration was calculated and normalized to the internal control C_6-ceramide.

Immunofluorescence analysis of LR clusters in CAECs

Individual LRs are too small (~50 nm) to be resolved by standard light microscopy, however, if raft components are crosslinked in living cells, clustered raft protein and lipid components can be visualized by fluorescence microscopy. For microscopic detection of LRs platforms, CAECs were grown on glass coverslips, transfected with siRNA as described above and treated with 10 ng/mL FasL for 15 min (Upstate, Charlottesville, VA) to induce clustering of lipid rafts. Cells were then washed in cold PBS and fixed for 15 min in 1% paraformaldehyde (PFA) in PBS, and blocked with 1% BSA in cell culture medium for 30 min. G_{M1} gangliosides enriched in LRs can be stained by FITC-labeled cholera toxin (FITC-CTX, 1 μg/ml, 15 min; Molecular Probes, Carlsbad, CA). Cells were extensively washed in cold PBS, fixed in 1% PFA for another 10 min, and mounted on glass slide with VECTSHIELD mounting media (Vector Laboratories, Inc., Burlingame, CA). Staining was visualized using a conventional Zeiss fluorescence microscope or a Leica TCS SP2 scanning confocal microscope. The patch formation of FITC-labeled CTX and gangliosides complex represented the clusters of lipid rafts. Clustering was defined as one or several intense spots of fluorescence on the cell surface, whereas unstimulated cells displayed a homogenous distribution of fluorescence throughout the membrane. In each experiment, the presence or absence of clustering in samples of 200 cells was scored by two independent observers. Results are given as the percentage of cells showing a cluster after the indicated treatment as described.

Isolation of LR-microdomains by gradient centrifugation

Cells were lysed in 1.5 ml MBS buffer containing (in mmol/L) morpholinoethane sulfonic acid, 25; NaCl, 150; EDTA, 1; PMSF, 1; Na_3VO_4, 1, and a cocktail of "complete" protease inhibitors (Roche, Nutley, NJ) and 1% Triton X-100, pH 6.5. Cell extracts were homogenized and LR microdomains were isolated as described previously (44).

Western blot analysis

For immunodetection of LR-associated proteins, 50 μl of resuspended proteins were subjected to SDS-PAGE (12% running gel), transferred onto a nitrocellulose membrane, and blocked as described (41). The membrane was probed with primary monoclonal antibodies: anti-β-actin, anti-flotillin-1, anti-gp91^{phox}, anti-p47^{phox} (1:1,000, BD Biosciences, San Jose, CA), anti-Fas (1:1,000, Upstate) or polyclonal antibody: anti-ASM or anti-NSM (1:1,000, Santa Cruz, Santa Cruz, CA) overnight at 4°C, followed by incubation with horseradish peroxidase-labeled anti-mouse or anti-rabbit IgG (1:5,000). The immunoreactive bands were detected by chemiluminescence methods (ECL, Pierce, Rockford, IL) and visualized on Kodak Omat film.

NADPH oxidase activity

The measurement of $O_2^{-\bullet}$ by ESR was followed as in our previous studies (46). Gently collected endothelial cells were suspended in modified Kreb's/HEPEs buffer containing 25 μmol/l of the metal chelator deferoximine. Approximately 1×10^6 CAECs were mixed with 1 mmol/L spin trap 1-hydroxy-3-methoxycarbonyl-2, 2,-5, 5-tetrame-thyl-pyrrolidine (CMH) in the presence or absence of 100 units/ml polyethylene glycol (PEG)-conjugated superoxide dismutase (SOD). The cell mixture loaded in glass capillaries was immediately analyzed by ESR (Noxygen Science Transfer & Diagnostics GmbH, Denzlingen, Germany) for production of $O_2^{-\bullet}$ at each minute for 10 min. The ESR settings were based on our previous studies. Next we analyzed the NADPH oxidase activity present in LR fractions from control and transfected cells by fluorescent spectrometry of DHE oxidation and DNA binding. Briefly, 50 μl of LR fractions were incubated with 100 μmol/L DHE and 0.5 mg/ml salmon test DNA (binds ethidium to amplify fluorescence signal) in 200 μl of PBS. NADPH (1 mmol/L) was added immediately before recording ethidium fluorescence by a fluorescence microplate reader (FLX800, Bio-Tek, Winoski, VT). The ethidium fluorescence increase (arbitrary unit) was used to represent NADPH oxidase activity (40, 44).

Statistics

Data are presented as means ± SE. Significant differences between and within multiple groups were examined using ANOVA for repeated measures, followed by Duncan's multiple-range test. Student's *t*-test was used to evaluate the significant differences between two groups of observations. $P < 0.05$ was considered statistically significant.

RESULTS

Effect of ASM gene silencing on FasL-induced ASM activation and increase in ceramide production in CAECs

To determine the efficiency of ASM gene silencing, ASM mRNA and protein expression levels were analyzed. As

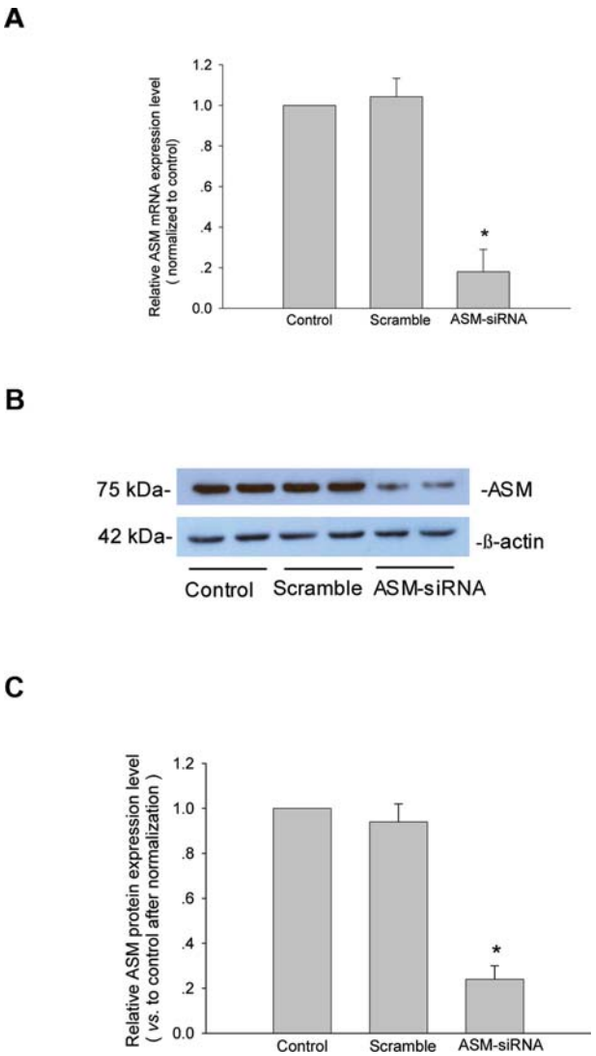

FIG. 1. Silencing of ASM in ECs. (**A**) Quantitative RT–PCR analysis mRNA levels of ASM in control, scrambled RNA, and ASM-siRNA transfected ECs. (**B**) Representative Western blot bands showing the protein level for ASM gene and β-actin. (**C**) Summarized data showing relative ASM protein levels in vehicle, scrambled RNA, and ASM-siRNA treated ECs after normalized to β-actin ($n = 6$).

shown in Fig. 1A, real time RT–PCR analysis revealed that ASM mRNA level was decreased by 86% in ASM-siRNA transfected CAECs, while Western blot analysis revealed that ASM protein levels were reduced by 75% in ASM-siRNA transfected cells after normalized to β-actin (Figs. 1B and 1C). In contrast, ASM mRNA and protein levels were not reduced in scrambled small RNA transfected CAECs. Similar efficiency was obtained for silencing of NSM in CAECs. It was found that that NSM mRNA level was decreased by 76% in NSM-siRNA transfected CAECs. Western blot analysis revealed that NSM protein levels were reduced by 72% in NSM-siRNA transfected cells (data not shown).

We also examined whether FasL-stimulated ASM activation and consequent increase in ceramide production can be blocked by siRNA silencing. In these experiments, CAECs were transfected with vehicle, scrambled small RNA or ASM-siRNA, and stimulated CAECs with 10 ng/mL FasL for 15 min, which was based on our previous studies (12, 42, 44). It was found that ASM-siRNA transfection significantly

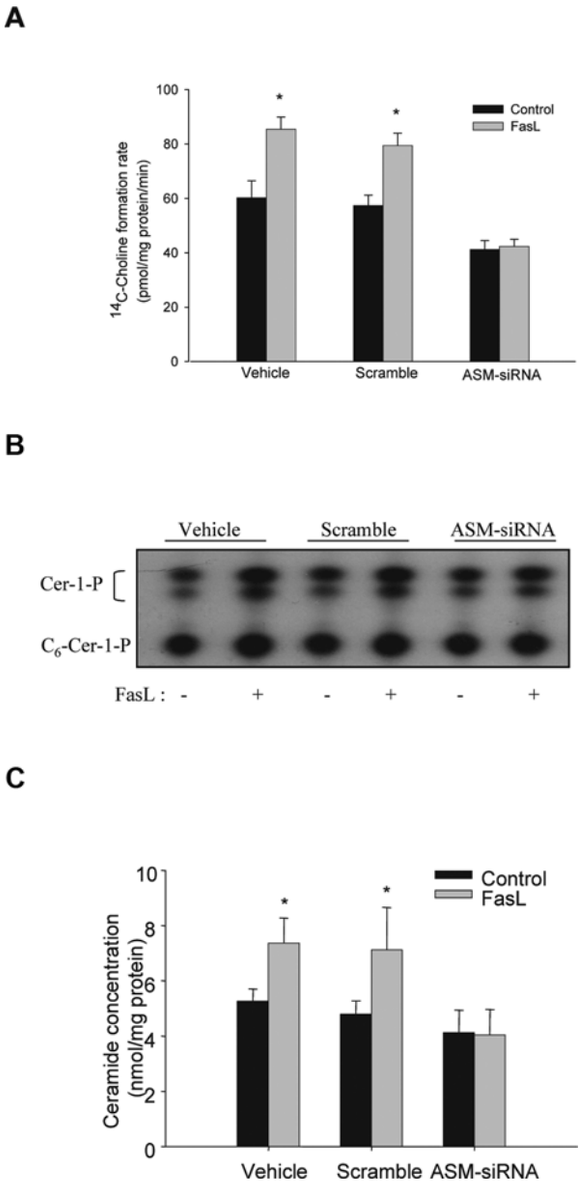

FIG. 2. Effect of FasL on the ASM activity and ceramide production in siRNA transfected CAECs. (**A**) Summarized data showing the conversion rate of ^{14}C-SM to ^{14}C-choline for measurement of ASM activity. (**B**) Representative autoradiograph of phospholipids fractionated by TLC after DG kinase assay. The bands represented ceramide-1-phosphate (Cer-1-P), which were from sample ceramide, and C6-cermaide-1-P (C6-Cer-1-P) from internal standard, respectively. (**C**) Summarized data showing quantitative changes in ceramide levels in ECs. The Cer-1-P and C6-Cer-1-P bands were scraped, and the radioactivity was counted using a liquid scintillation counter. Cer-1-P level was normalized to C6-Cer-1-P. *$p < 0.05$ vs. control ($n = 6$).

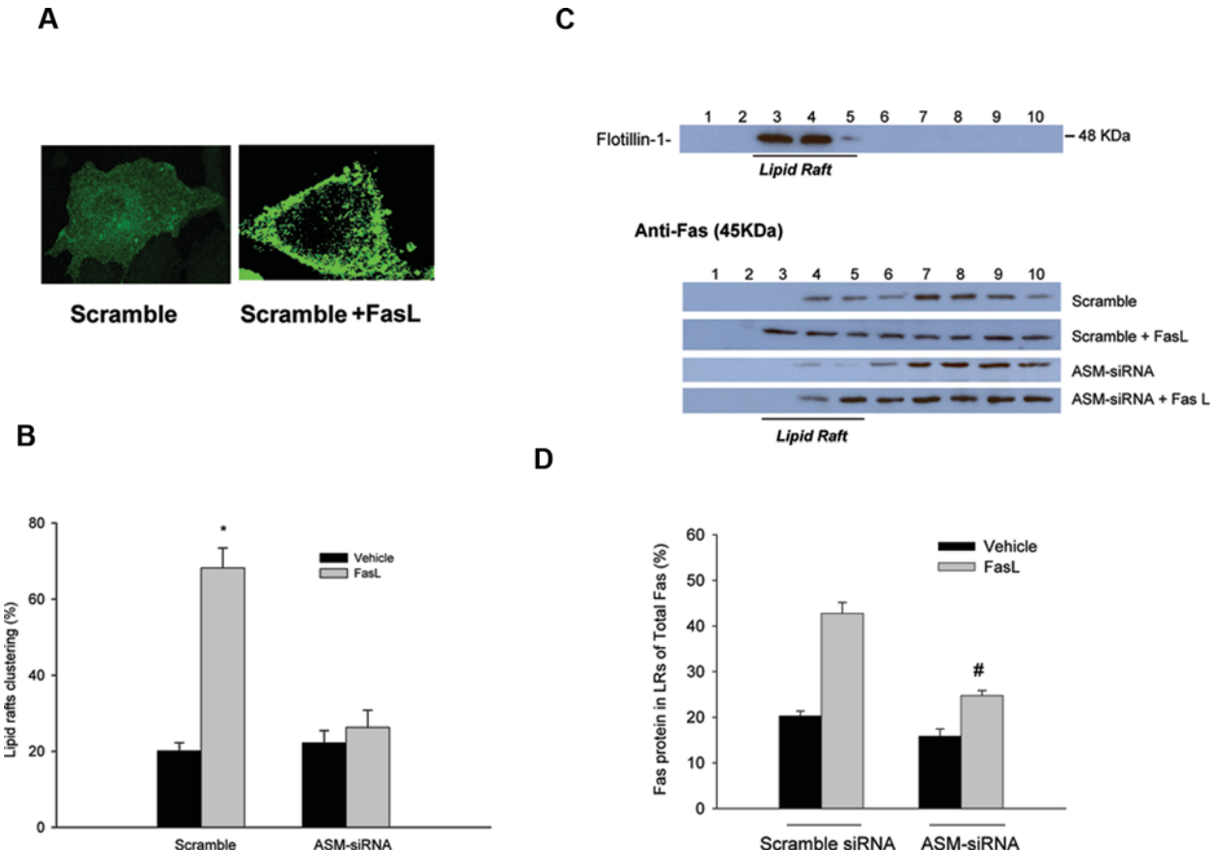

FIG. 3. Effect of ASM silencing on FasL-induced LR clustering and Fas aggregation on EC membrane. (**A**) Representative confocal microscopic images show LR clustering after stimulation with FasL on the membrane of ECs. (**B**) Summarized data showing the effect of FasL on the percentage of cells with intense LR clusters in scrambled small RNA or ASM-siRNA treated ECs ($n = 6$). (**C**) Western blot analysis showing LR-enriched fractions #3–5 by probing with flotillin-1 antibody and the distribution of Fas in the scrambled small RNA or ASM-siRNA transfected ECs with or without FasL stimulation. (**D**): Summarized data showing the ratio of Fas in LR fractions from total Fas in these ECs. *$p < 0.05$ vs. scrambled RNA control; #$p < 0.05$ vs. scrambled RNA+FasL ($n = 6$).

decreased basal ASM activity by 51% and completely abolished FasL stimulated ASM activation (Fig. 2A).

Figure 2B presents a typical TLC autoradiogram showing ceramide levels measured as ceramide-1-P in CAECs under control condition and after incubation with FasL. Ceramide consists of a long-chain or sphingoid base linked to a fatty acid via an amide bond. Most natural ceramides have a long acyl chain typically with 16–24 carbon atoms. As shown, the upper two bands indicate the ceramide mixtures and the lower band stands for the internal control, C_6-ceramide. After normalized to internal control, C_6-ceramide, the basal ceramide concentrations in vehicle, scrambled small RNA, and ASM-siRNA transfected CAECs were 5.2 ± 0.2, 4.8 ± 0.5, and 4.2 ± 0.8 (in nmol/mg protein), respectively. FasL led to a 40% and 48% increase in ceramide levels in vehicle and scrambled small RNA treated CAECs. However, this increase in the ceramide level was not observed in ASM-siRNA tranfected cells (Fig. 2C).

In parallel, gene silencing of NSM by siRNA was also performed. It was found that NSM-siRNA had no effect on FasL-induced ASM activity and ceramide production (data not shown).

Effects of ASM gene silencing on FasL-induced LR clustering in the membrane of CAECs

To examine whether ASM-ceramide signaling is involved in the LR clustering and formation of redox signaling platform, CAECs were treated with siRNA, stained with FITC-CTX, and the distribution of FITC-CTX labeled LR patches was visualized on the cell membrane. As shown in Fig. 3A, in scrambled small RNA transfected CAECs, LRs were evenly spread throughout the cell membrane under control condition as indicated by weak diffused FITC fluorescence (Scramble). Upon stimulation with FasL, these endothelial LRs formed multiple patches on the cell membrane as displayed by large and intense fluorescence patches (Scramble+FasL). However, the FasL-stimulated increase in fluorescence patches was not observed in ASM-siRNA treated cells. Figure 3B summarizes the effects of FasL on the LR clustering in cell membranes by

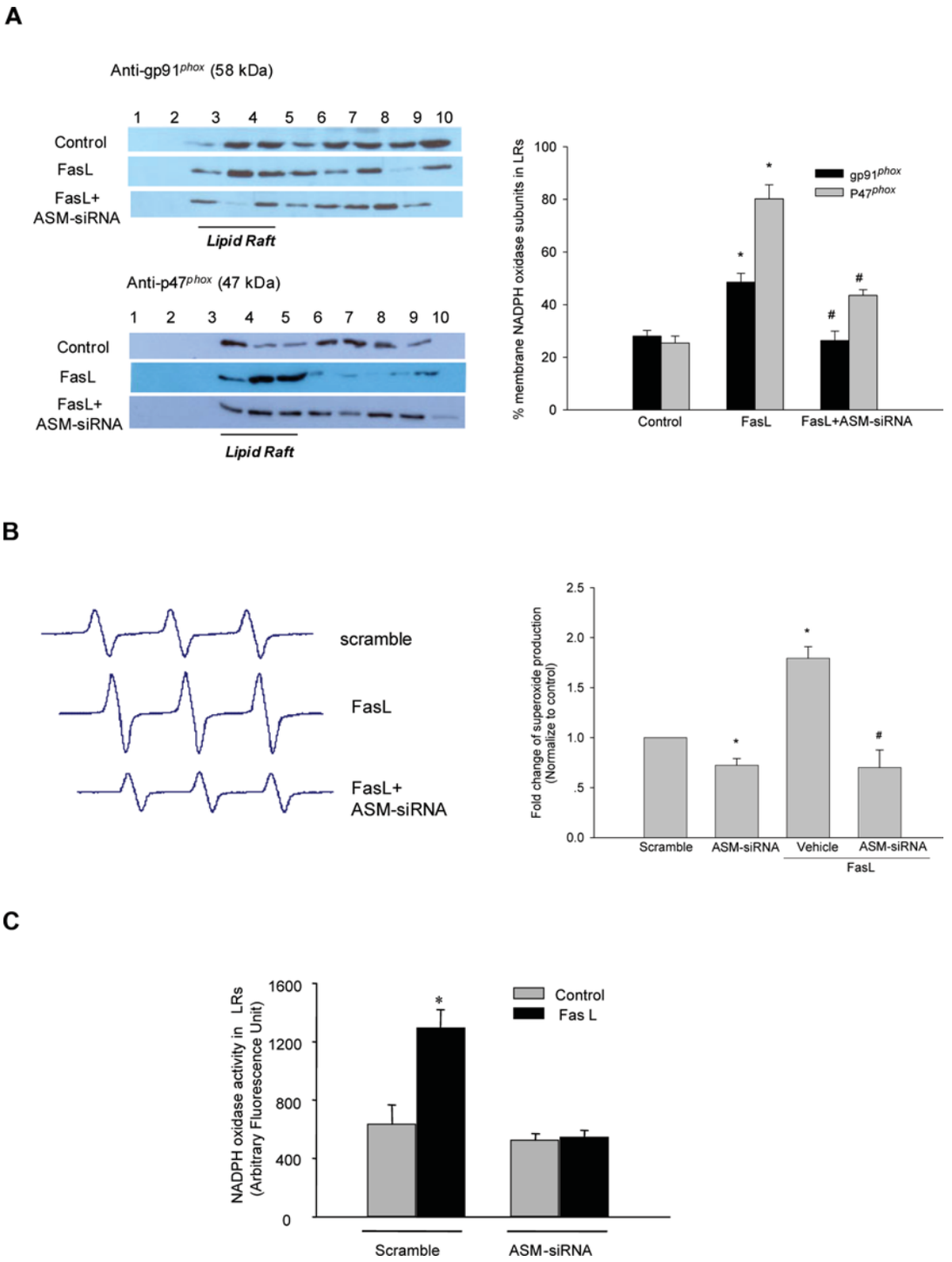

FIG. 4. Effect of ASM silencing on FasL-induced NAD(P)H oxidase activity in LRs in ECs. (**A**) Shown are the blot patterns (*left panels*) for gp91^{phox} and p47^{phox} on the membrane in ECs treated with scrambled small RNA (control), scrambled small RNA with FasL stimulation (FasL) or ASM-siRNA with FasL stimulation (ASM-siRNA+FasL). *Right panel* is summarized data for the percentage of protein content in LRs. (**B**) Representative ESR spectra showing SOD-inhibitable $O_2^{-\bullet}$ signals (*left*) and summarized data depicting $O_2^{-\bullet}$ production in CAECs with different treatments ($n = 6$). (**C**) Summarized data showing NADPH-dependent $O_2^{-\bullet}$ production using DHE fluorescence assay in LR fractions (collect fractions 3–5). *$p < 0.05$ vs. control; #$p < 0.05$ vs. FasL ($n = 6$).

counting these LR patches. In scrambled small RNA treated CAECs, there were 24% of the cells displayed with intense LR clusters under resting condition, while 73% of the cells showed clustering of LR after stimulation with FasL. Treatment of CAECs with ASM-siRNA prevented LR-clustering and FasL only increased the number of cells with intense LR clusters from 25% to 32%.

Effects of ASM gene silencing on FasL-induced Fas aggregation in isolated LR fractions in CAECs

As shown in Fig. 3C, Western blot analysis showed that the fractions 3–5 are the only fractions immunoreactive to flotillin-1, which is a specific marker for LRs. Therefore, these three fractions were designated as LR-enriched fractions. Furthermore, Fas, a 45 kDa protein, could be detected in most of the membrane fractions isolated from CAECs treated with scrambled small RNA under control condition. When these cells were treated by FasL, there was a marked increase in Fas protein amount in LR-enriched fractions. However, this increase was significantly reduced by ASM-siRNA silencing. The percent change of Fas protein in LR-enriched fractions is summarized in Fig. 3D.

Role of ASM-mediated formation of LR platforms in recruitment of NAD(P)H oxidase subunits and activation of this enzyme in CAECs

Figure 4A presents typical blots and summarized data showing the distribution of $gp91^{phox}$ and $p47^{phox}$ in isolated LR-enriched fractions from CAECs. In the cells treated with scrambled small RNA (control), FasL increased the amount of $gp91^{phox}$ protein present in LR-enriched fractions by 68%, which was completely blocked by ASM-siRNA. Meanwhile, FasL induced a three-fold increase of $p47^{phox}$, a cytosolic subunit of NAD(P)H oxidase, in LR-enriched fractions of cells, whereas ASM-siRNA treatment markedly attenuated FasL-induced recruitment of $p47^{phox}$ to the membrane. We also analyzed NAD(P)H oxidase activity by measurement of $O_2^{-\bullet}$ production using ESR. As shown in Fig. 4B, we found that FasL significantly increased $O_2^{-\bullet}$ in CAECs by 79%, which could not be observed in ASM-siRNA transfected CAECs. Next, we analyzed NAD(P)H oxidase activity as an indicator for NADPH-dependent $O_2^{-\bullet}$ production in isolated LR-enriched fractions by fluorescent spectrometry using DHE as indicator for NADPH-dependent $O_2^{-\bullet}$ production. As summarized in Fig. 4C, FasL (10 ng/ml) doubled membrane NAD(P)H oxidase activity in isolated LR-enriched fractions, which was abolished in ASM-siRNA treated cells.

Effects of SOD on FasL-induced ASM activity and LR clustering

Recent studies has shown that $O_2^{-\bullet}$ or other ROS can alter ceramide level in cells through their action on SMs. It is interesting to know whether ROS derived from ASM/ceramide triggered LR redox signaling platforms can feedback regulate the ASM activity. Therefore, we examined the effect of SOD on FasL-stimulated ASM activation and consequent LR clustering. It was found that FasL-induced ASM activity was abolished by SOD (150 units/ml) (Fig. 5) and the enhanced LR clustering by FasL was not observed in CAECs pretreated with SOD (Fig. 6). Therefore, we suggested that FasL-induced $O_2^{-\bullet}$ may be involved in this regulatory mechanism.

Effects of $O_2^{-\bullet}$ production induced by xanthine/xanthine oxidase (X/XO) on ASM activity

To further confirm whether enhanced ROS in LR redox signaling platforms can act on ASM to increase its activity, CAECs were incubated with an exogenous $O_2^{-\bullet}$ generating system, xanthine/xanthine oxidase (X/XO, 40 μM/0.1 mU/ml) for 15 min and then ASM activity was examined. As shown in Fig. 7A, both X/XO and X/XO + FasL significantly increased ASM activity, and this enhanced ASM activity was abolished by SOD. Combined with the results from Fig. 5, it seems that FasL and X/XO shares a similar mechanism to increase ASM activity and $O_2^{-\bullet}$ is involved in this regulatory mechanism.

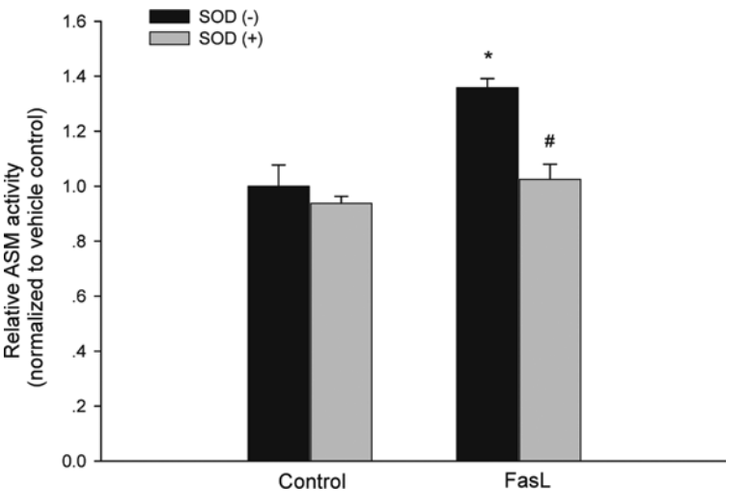

FIG. 5. Effect of SOD on the regulation ASM activity on EC membrane. Summarized data showing fold change of the conversion rate of ^{14}C-SM to ^{14}C-choline for measurement of ASM activity by FasL stimulation with or without SOD pretreatment. *$p < 0.05$ vs. control; #$p < 0.05$ vs. FasL ($n = 6$).

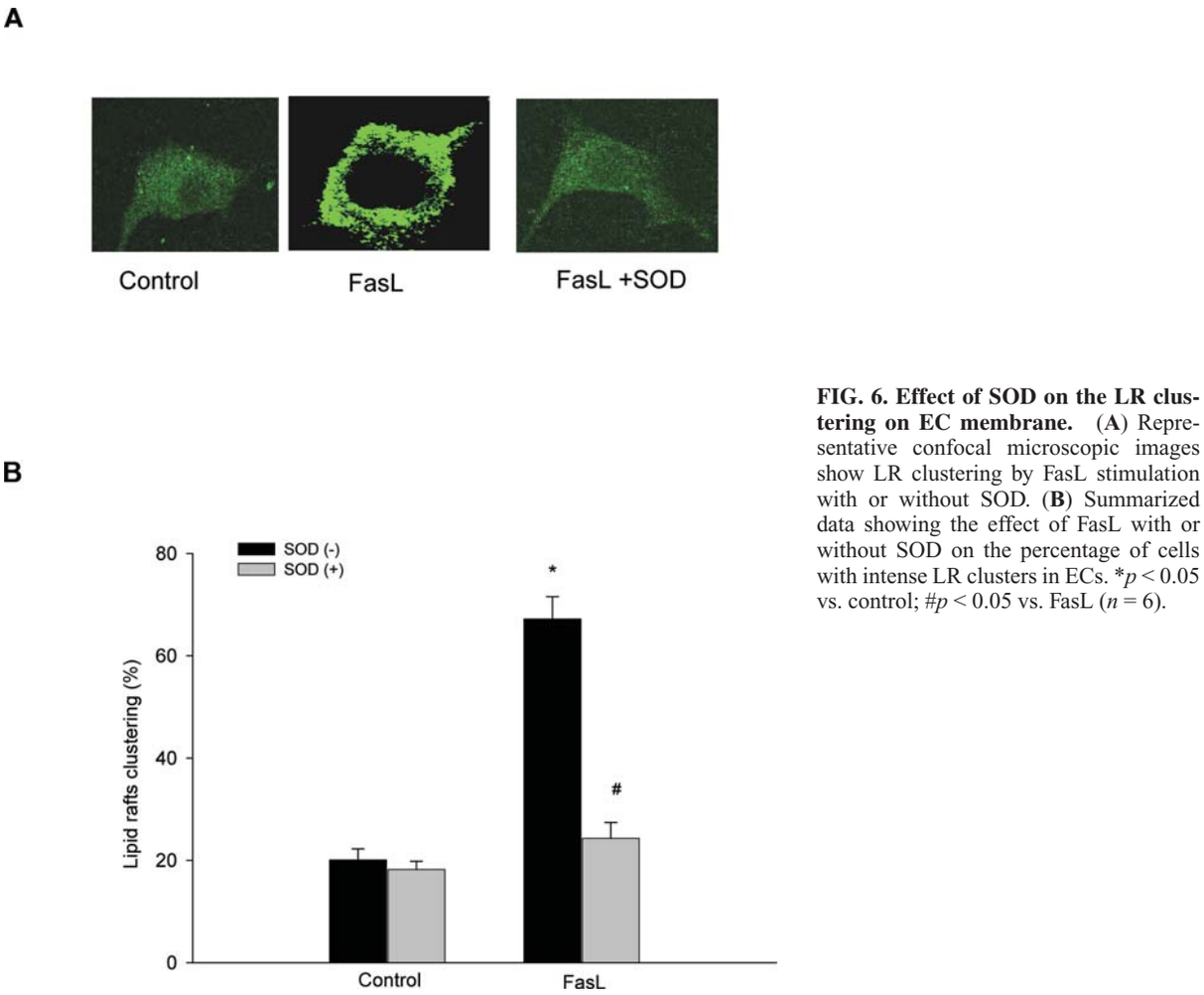

FIG. 6. Effect of SOD on the LR clustering on EC membrane. (**A**) Representative confocal microscopic images show LR clustering by FasL stimulation with or without SOD. (**B**) Summarized data showing the effect of FasL with or without SOD on the percentage of cells with intense LR clusters in ECs. $*p < 0.05$ vs. control; $\#p < 0.05$ vs. FasL ($n = 6$).

Effects of xanthine/xanthine oxidase (X/XO) on LR clustering

As shown in Fig. 7B, it was found that X/XO dramatically increased LR clustering in the membrane of CAECs as FasL did. More interestingly, co-treatment of the cells with FasL and X/XO enhanced the formation of fluorescence CTX-labeled patches (LR clustering) in comparison with X/XO or FasL treatment alone. However, the enhanced LR clustering was not observed in CAECs pretreated with SOD. Figure 7B summarized the effects of X/XO or X/XO + FasL on the LR clustering in cell membranes by counting these LR patches with or without SOD treatment. Positive cells with patch formation during incubation with FasL were significantly increased in the presence of X/XO, which could be blocked by SOD. It is clear that $O_2^{-\bullet}$ is involved in FasL-induced LR clustering.

DISCUSSION

In the present study, we examined the role of ASM-ceramide pathway and its redox amplification in mediating FasL-induced formation of LR redox signaling platforms in the endothelial cell membrane. By using siRNA to knock down ASM gene, we successfully inhibited the expression of this enzyme and attenuated FasL-induced activation of ASM and release of ceramide in CAECs. Furthermore, ASM gene silencing blocked FasL-induced formation of LR clustering and aggregation of NAD(P)H oxidase subunits in these LR clusters of CAECs. This formation of LR redox signaling platforms enhances $O_2^{-\bullet}$ production from endothelial cells in response to FasL stimulation. Finally, we found that X/XO increased ASM activity and consequent LR clustering, which were blocked by SOD. All these together indicate that there is a redox signaling network in coronary arterial endothelial cell that can be initiated by ASM and enhanced by redox feedforwarding regulation.

Previous studies have demonstrated that ASM-deficient cells isolated from Niemann–Pick disease Type (NPDA) patients with an inborn defect of ASM or from ASM knockout mice were resistant to Fas or TNF initiated apoptosis (8, 24, 25, 28). Our laboratories have recently shown that FasL activates ASM, but not NSM, and thereby increases ceramide levels in CAECs (42). We recently found that FasL induced a LR clustering with aggregation of NAD(P)H oxidase subunits, forming a LR redox signaling platform and

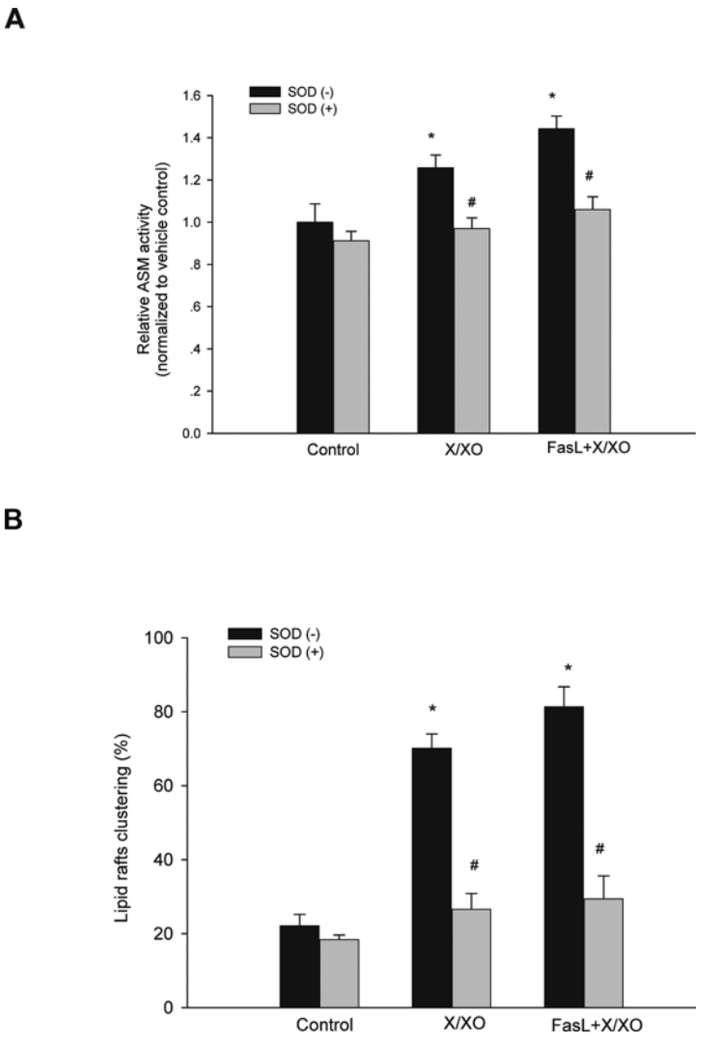

FIG. 7. Effect of $O2^{-\bullet}$ on the regulation of ASM activity and LR clustering on EC membrane. (**A**) Summarized data showing fold change of the conversion rate of ^{14}C-SM to ^{14}C-choline for measurement of ASM activity with different stimuli including X/XO, X/XO+FasL with or without SOD pretreatment. (**B**) Summarized data showing the effect of X/XO, X/XO+FasL with or without SOD on the percentage of cells with intense LR clusters in ECs. *$p < 0.05$ vs. control; #$p < 0.05$ vs. different stimuli ($n = 6$).

causing endothelial dysfunction (44). To further study the role of ASM in the formation of LR redox signaling platform and subsequent endothelial function, the present study used RNA interference to knockdown ASM and NSM genes, two major forms of SM in CAECs. This RNA interference approach is considered as a more specific and powerful methodology than traditional pharmacological interventions, which may more definitively define the role of this lipid signaling pathway in the regulation of endothelial function. It was found that FasL induced increase in ASM activity rather than NSM activity and that this FasL-induced ceramide production was abolished in ASM-siRNA transfected cells. However, NSM-silencing had no effects on FasL-induced ceramide production. These results strongly support a view that FasL stimulates endogenous ceramide production via activation of ASM in CAECs. It should be noted that the basal ceramide level was not significantly decreased by ASM-siRNA, which may be due to a compensation response by *de novo* ceramide synthesis or downregulation of ceramidase-mediated degradation of ceramide during a relatively long time period. These results also indicate that gene silencing using siRNA strategy is particularly suitable for studies on acute response of ASM to stimuli such as FasL. Using this RNA interference strategy, we determined the importance of ASM in mediating or modulating the formation of LR signaling platforms in coronary endothelial cells. It was found that FasL-induced LR clustering was abolished in the cell membrane of ASM gene-silenced CAECs, but not altered in NSM gene-slienced CAECs, suggesting that it is ASM product, ceramide which may contribute to the formation of LR platforms in these endothelial cells, which is consistent with previous studies showing that ceramide was capable of triggering the fusion of LRs into larger platforms in the membrane of different cell types (12, 13, 15, 36).

It has been reported that clustering of receptors in LR-derived platforms upon stimulation is a common mechanism for initiation of transmembrane signaling. Clustering or recruitments of various receptors during LR clustering importantly participate in the regulation of a variety of cell functions (15, 34). For example, clustering of Fas has been found in lymphocytes, liver cells, and endothelial cells, which is the

prerequisite for signal transduction of death receptors and apoptosis (15, 16). In addition, this ceramide-enriched membrane platform has been shown to be involved in clustering of other receptors such as CD20, CD40, tumor necrosis factor receptor (TNFR), and epidermal growth factor receptor (EGFR) (4, 13, 20). In the present study, we found that Fas protein levels in LR fractions in ECs treated with FasL was markedly increased, which could be substantially blocked by ASM gene silencing. These results indicate that FasL induced LR clustering associated with ASM activation in endothelial cells also leads to aggregation or recruitment of related receptor such as Fas. This ceramide-mediated aggregation of Fas in LR platforms may be associated with the preference of these receptors in ceramide-enriched LRs and the interaction of LRs with Fas (19, 29, 37).

It is well known that NAD(P)H oxidase-mediated redox signaling importantly contributes to the regulation of endothelial function and cellular activities in many other mammalian cells (7, 21, 32, 35). Activation of this redox signaling enzyme is dependent on the assembly of its subunits when cells are stimulated by different challenges. However, so far it remains unknown how these NAD(P)H oxidase subunits are assembled or aggregated in response to the activation of death receptors. In recent studies, we and others reported that the formation of LR-derived platforms is linked to NAD(P)H oxidase activation in response to FasL, endostatin, and vascular endothelial growth factor (VEGF) (39, 44). Therefore, this LR platform formation may represent one of the important mechanism mediating NAD(P)H oxidase assembling and activation in endothelial cells. The present study further explored the mechanism by which this LR related activation of NAD(P)H oxidase occurs and produces functional alterations with a focus on the role of ceramide-enriched microdomains. It was found that in ASM-siRNA transfected CAECs the levels of $gp91^{phox}$ and $p47^{phox}$ clustered in LR microdomains were substantially decreased accompanied by significantly decreased NAD(P)H oxidase activity compared to the cells transfected with scrambled RNA controls. It is suggested that aggregation of NAD(P)H oxidase subunits such as $gp91^{phox}$ and $p47^{phox}$ in the LR clusters are associated with ASM-mediated ceramide production. These results provide evidence that ASM-ceramide signaling pathway is involved in the redox regulation of endothelial function via activation of NAD(P)H oxidase clustered in the LR platforms.

Recently, it has been reported that ROS and nitric oxide synthases (NOS) are involved in sphingolipid metabolism (38). On the other hand, sphingolipids including ceramide, sphingosine, and sphingosine-1-phosphate are able to regulate cellular redox homeostasis through regulation of NAD(P)H oxidase, mitochondrial integrity, NOS and antioxidant enzymes (11, 38, 41, 45). Therefore, it is interesting to know whether ROS derived from ASM/ceramide triggered LR redox signaling platforms can feedback regulate the ASM activity or ceramide production. In the present study, we did show that SOD decreased, but X/XO, an exogenous $O_2^{-\bullet}$ generating system increased ASM activity and LR clustering in the membrane of CAECs. Furthermore, co-treatment of these cells with FasL and X/XO produce additive effect on ASM activity and LR clustering, which was blockable by SOD. It is suggested that a redox regulation of ASM in LR redox signaling platforms occurs and in this way ASM activation is increased, whereby ceramide is produced more and more, resulting in amplification of this LR induced redox signaling. This study did not attempted to address how ROS stimulates ASM activity and lead to ceramide production since there are some reports indicating that oxidants may dimerize ASM and thereby enhance its activity (5, 31). In this regard, Qiu *et al*. reported that the formation of ASM dimer due to modification of the free C-terminal cysteine by oxidants significantly enhanced the activity of this enzyme. A "cysteine switch" activation mechanism is proposed by this research group to interpret the enhancement of ASM activity by oxidants. It is assumed that the free C-terminal cysteine involved zinc coordination of the active size may be destroyed due to loss of free cysteine. In fact, the dimerization of enzyme molecules induced by ROS is now considered as one of the important mechanisms mediating the effect of ROS on cellular enzyme activity (3, 9, 43). In addition to the action of this protein modification, there is evidence that SM peroxidation could also promote the formation of large rafts in bilayer vesicle experiments (2). Moreover, ROS-induced activation of certain regulatory enzymes may also contribute to this feedforwarding amplification of LR platform formation**.** For example, Src kinases have been reported to be activated by ROS and then move into LR clusters. Activated Src may cause transphosphorylation, resulting in activation of related enzymes in LR clusters and thereby producing a feedforward regulation in the formation of LR signaling platforms (30).

In summary, the present study demonstrated that FasL-induced activation of ASM and production of ceramide result in the formation of LR-derived signaling platforms, which could be blocked by silencing ASM gene in CAECs. Aggregation or recruitment of NAD(P)H oxidase subunits in these LR platforms constitutes a redox signaling complex, which produce $O_2^{-\bullet}$. Through a feedforwarding mechanism, $O_2^{-\bullet}$ and corresponding ROS in the LR redox signaling platforms may enhance ASM activity and promote further formation of LRs clusters. Therefore, ASM and $O_2^{-\bullet}$ interactions constitute a redox signaling network via LR clustering to conduct signal transduction and thereby mediate the actions of death receptor activation in coronary endothelial cells.

ACKNOWLEDGMENT

This study was supported by grants from the National Institute of Health (HL-57244, HL-70726, DK-54927) and Predoctoral Fellowship 0410061Z (to A.Y. Zhang).

ABBREVIATIONS

ASM, acid sphingomyelinase; BSA, bovine serum albumin; CAECs, coronary arterial endothelial cells; EGFR, epidermal growth factor receptor; FasL, Fas ligand; FCS, fetal calf serum; H&E, hematoxylin and eosin; LR, lipid raft; NPDA, Niemann–Pick disease Type; NSM, neutral sphingomyelinases; $O_2^{-\bullet}$, superoxide; PFA, paraformaldehyde; siRNA, small interference RNA; SOD, superoxide dismutase;

TNFR, tumor necrosis factor receptor; VGF, vascular endothelial growth factor; X/XO, xanthine/xanthine oxidase.

REFERENCES

1. Alliegro MC. Effects of dithiothreitol on protein activity unrelated to thiol-disulfide exchange: for consideration in the analysis of protein function with Cleland's reagent. *Anal Biochem* 282: 102–106, 2000.
2. Ayuyan AG and Cohen FS. Lipid peroxides promote large rafts: effects of excitation of probes in fluorescence microscopy and electrochemical reactions during vesicle formation. *Biophys J* 91: 2172–2183, 2006.
3. Berruet L, Muller–Steffner H, and Schuber F. Occurrence of bovine spleen CD38/NAD+glycohydrolase disulfide-linked dimers. *Biochem Mol Biol Int* 46: 847–855, 1998.
4. Bezombes C, Grazide S, Garret C, Fabre C, Quillet–Mary A, Muller S, Jaffrezou JP, and Laurent G. Rituximab antiproliferative effect in B-lymphoma cells is associated with acid-sphingomyelinase activation in raft microdomains. *Blood* 104: 1166–1173, 2004.
5. Bollinger CR, Teichgraber V, and Gulbins E. Ceramide-enriched membrane domains. *Biochim Biophys Acta* 1746: 284–294, 2005.
6. Brown DA and London E. Functions of lipid rafts in biological membranes. *Annu Rev Cell Dev Biol* 14: 111–136, 1998.
7. Cai H. NAD(P)H oxidase-dependent self-propagation of hydrogen peroxide and vascular disease. *Circ Res* 96: 818–822, 2005.
8. De Maria R, Rippo MR, Schuchman EH, and Testi R**.** Acidic sphingomyelinase (ASM) is necessary for fas-induced GD3 ganglioside accumulation and efficient apoptosis of lymphoid cells. *J Exp Med* 187: 897–902, 1998.
9. Finkel T. Signal transduction by reactive oxygen species in nonphagocytic cells. *J Leukoc Biol* 65: 337–340, 1999.
10. Fullekrug J and Simons K. Lipid rafts and apical membrane traffic. *Ann NY Acad Sci* 1014: 164–169, 2004.
11. Garcia–Ruiz C, Colell A, Mari M, Morales A, and Fernandez–Checa JC. Direct effect of ceramide on the mitochondrial electron transport chain leads to generation of reactive oxygen species. Role of mitochondrial glutathione. *J Biol Chem* 272: 11369–11377, 1997.
12. Grassme H, Jekle A, Riehle A, Schwarz H, Berger J, Sandhoff K, Kolesnick R, and Gulbins E. CD95 signaling via ceramide-rich membrane rafts. *J Biol Chem* 276: 20589–20596, 2001.
13. Grassme H, Jendrossek V, Bock J, Riehle A, and Gulbins E. Ceramide-rich membrane rafts mediate CD40 clustering. *J Immunol* 168: 298–307, 2002.
14. Grassme H, Schwarz H, and Gulbins E. Molecular mechanisms of ceramide-mediated CD95 clustering. *Biochem Biophys Res Commun* 284: 1016–1030, 2001.
15. Gulbins E and Grassme H. Ceramide and cell death receptor clus tering. *Biochim Biophys Acta* 1585: 139–145, 2002.
16. Gulbins E and Kolesnick R. Acid sphingomyelinase-derived ceramide signaling in apoptosis. *Subcell Biochem* 36: 229–244, 2002.
17. Gulbins E and Kolesnick R. Raft ceramide in molecular medicine. *Oncogene* 22: 7070–7077, 2003.
18. Holopainen JM, Subramanian M, and Kinnunen PK. Sphingomyelinase induces lipid microdomain formation in a fluid phosphatidylcholine/sphingomyelin membrane. *Biochemistry* 37: 17562–17570, 1998.
19. Hostager BS, Catlett IM, and Bishop GA. Recruitment of CD40 and tumor necrosis factor receptor-associated factors 2 and 3 to membrane microdomains during CD40 signaling. *J Biol Chem* 275: 15392–15398, 2000.
20. Huang Y, Yang J, Shen J, Chen FF, and Yu Y. Sphingolipids are involved in *N*-methyl-*N*'-nitro-*N*-nitrosoguanidine-induced epidermal growth factor receptor clustering. *Biochem Biophys Res Commun* 330: 430–438, 2005.
21. Ikeda S, Ushio–Fukai M, Zuo L, Tojo T, Dikalov S, Patrushev NA, and Alexander RW. Novel role of ARF6 in vascular endothelial growth factor-induced signaling and angiogenesis. *Circ Res* 96: 467–475, 2005.
22. Janes PW, Ley SC, Magee AI, and Kabouridis PS. The role of lipid rafts in T cell antigen receptor (TCR) signalling. *Semin Immunol* 12: 23–34, 2000.
23. Kabouridis PS. Lipid rafts in T cell receptor signalling. *Mol Membr Biol* 23: 49–57, 2006.
24. Kirschnek S, Paris F, Weller M, Grassme H, Ferlinz K, Riehle A, Fuks Z, Kolesnick R, and Gulbins E. CD95-mediated apoptosis in vivo involves acid sphingomyelinase. *J Biol Chem* 275: 27316–27323, 2000.
25. Lozano J, Menendez S, Morales A, Ehleiter D, Liao WC, Wagman R, Haimovitz–Friedman A, Fuks Z, and Kolesnick R. Cell autonomous apoptosis defects in acid sphingomyelinase knockout fibroblasts. *J Biol Chem* 276: 442–448, 2001.
26. Matsumoto A, Comatas KE, Liu L, and Stamler JS. Screening for nitric oxide-dependent protein–protein interactions. *Science* 301: 657-661, 2003.
27. Natoli G, Costanzo A, Guido F, Moretti F, and Levrero M. Apoptotic, non-apoptotic, and anti-apoptotic pathways of tumor necrosis factor signalling. *Biochem Pharmacol* 56: 915–920, 1998.
28. Paris F, Grassme H, Cremesti A, Zager J, Fong Y, Haimovitz–Friedman A, Fuks Z, Gulbins E, and Kolesnick R. Natural ceramide reverses Fas resistance of acid sphingomyelinase(-/-) hepatocytes. *J Biol Chem* 276: 8297–8305, 2001.
29. Pfeiffer A, Bottcher A, Orso E, Kapinsky M, Nagy P, Bodnar A, Spreitzer I, Liebisch G, Drobnik W, Gempel K, Horn M, Holmer S, Hartung T, Multhoff G, Schutz G, Schindler H, Ulmer AJ, Heine H, Stelter F, Schutt C, Rothe G, Szollosi J, Damjanovich S, and Schmitz G. Lipopolysaccharide and ceramide docking to CD14 provokes ligand-specific receptor clustering in rafts. *Eur J Immunol* 31: 3153–3164, 2001.
30. Powers KA, Szaszi K, Khadaroo RG, Tawadros PS, Marshall JC, Kapus A, and Rotstein OD. Oxidative stress generated by hemorrhagic shock recruits Toll-like receptor 4 to the plasma membrane in macrophages. *J Exp Med* 203: 1951–1961, 2006.
31. Qiu H, Edmunds T, Baker–Malcolm J, Karey KP, Estes S, Schwarz C, Hughes H, and Van Patten SM. Activation of human acid sphingomyelinase through modification or deletion of C-terminal cysteine. *J Biol Chem* 278: 32744–32752, 2003.
32. Shao D, Segal AW, and Dekker LV. Lipid rafts determine efficiency of NADPH oxidase activation in neutrophils. *FEBS Lett* 550: 101–106, 2003.
33. Simons K and Ikonen E. Functional rafts in cell membranes. *Nature* 387: 569–572, 1997.
34. Simons K and Toomre D. Lipid rafts and signal transduction. *Nat Rev Mol Cell Biol* 1: 31–39, 2000.
35. Touyz RM. Lipid rafts take center stage in endothelial cell redox signaling by death receptors. *Hypertension* 47: 16–18, 2006.
36. van Blitterswijk WJ, van der Luit AH, Veldman RJ, Verheij M, and Borst J. Ceramide: second messenger or modulator of membrane structure and dynamics? *Biochem J* 369: 199–211, 2003.
37. Vidalain PO, Azocar O, Servet–Delprat C, Rabourdin–Combe C, Gerlier D, and Manie S. CD40 signaling in human dendritic cells is initiated within membrane rafts. *EMBO J* 19: 3304–3313, 2000.
38. Won JS and Singh I. Sphingolipid signaling and redox regulation. *Free Radic Biol Med* 40: 1875–1888, 2006.
39. Yang B and Rizzo V. TNF{alpha} potentiates protein-tyrosine nitration through activation of NADPH oxidase and eNOS localized in membrane rafts and caveolae of bovine aortic endothelial cells. *Am J Physiol Heart Circ Physiol* 292: H954–962, 2007.
40. Yi F, Zhang AY, Janscha JL, Li PL, and Zou AP. Homocysteine activates NADH/NADPH oxidase through ceramide-stimulated Rac GTPase activity in rat mesangial cells. *Kidney Int* 66: 1977–1987, 2004.
41. Yi F, Zhang AY, Li N, Muh RW, Fillet M, Renert AF, and Li PL. Inhibition of ceramide-redox signaling pathway blocks glomerular injury in hyperhomocysteinemic rats. *Kidney Int* 70: 88–96, 2006.
42. Zhang AY, Teggatz EG, Zou AP, Campbell WB, and Li PL. Endostatin uncouples NO and Ca2+ response to bradykinin through enhanced O2*- production in the intact coronary endothelium. *Am J Physiol Heart Circ Physiol* 288: H686–694, 2005.

43. Zhang AY, Yi F, Teggatz EG, Zou AP, and Li PL. Enhanced production and action of cyclic ADP-ribose during oxidative stress in small bovine coronary arterial smooth muscle. *Microvasc Res* 67: 159–167, 2004.
44. Zhang AY, Yi F, Zhang G, Gulbins E, and Li PL. Lipid raft clustering and redox signaling platform formation in coronary arterial endothelial cells. *Hypertension* 47: 74–80, 2006.
45. Zhang DX, Zou AP, and Li PL. Ceramide-induced activation of NADPH oxidase and endothelial dysfunction in small coronary arteries. *Am J Physiol Heart Circ Physiol* 284: H605–612, 2003.
46. Zhang G, Zhang F, Muh R, Yi F, Chalupsky K, Cai H, and Li PL. Autocrine/paracrine pattern of superoxide production through NAD(P)H oxidase in coronary arterial myocytes. *Am J Physiol Heart Circ Physiol* 292: H483–495, 2007.

Address reprint requests to:
Pin-Lan Li, M.D, Ph.D.
Department of Pharmacology and Toxicology
Medical College of Virginia
Virginia Commonwealth University
410 N 12th Street
Richmond, VA 23298

E-mail: pli@vcu.edu

Date of first submission to ARS Central, November 17, 2006; date of final revised submission, February 10, 2007; date of acceptance, February 14, 2007.